Journal of Applied Polymer Science

Synthesis of Star Polymer Poly(ethylene glycol)$_3$–Poly(*N,N*-dimethyl acrylamide) and Its Application in Protein Resistance and Separation

Jinxing Xing, Lin Tan, Fuhu Cao, Yanmei Wang

Chinese Academy of Sciences, Key Laboratory of Soft Matter Chemistry, Department of Polymer Science and Engineering, University of Science and Technology of China, Hefei 230026, People's Republic of China

Correspondence to: Y. Wang (E-mail: wang@ustc.edu.cn)

ABSTRACT: A star polymer composed of three poly(ethylene glycol) (PEG) arms and one poly(*N,N*-dimethyl acrylamide) (PDMA) arm (PEG$_3$–PDMA) was synthesized by amidation and atom-transfer radical polymerization. The structure of PEG$_3$–PDMA was confirmed by ^{1}H-NMR and gel permeation chromatography results. The surface adsorption and protein-resistance behaviors of the star polymer PEG$_3$–PDMA, diblock copolymer PEG–PDMA, and homopolymer PEG were investigated by a quartz crystal microbalance with dissipation. The results indicate that the PEG$_3$–PDMA coating could reduce protein adsorption to 13% at least, more effectively than the PEG–PDMA coating; this indicated that the protein-resistance properties depended on the PEG chain density and surface coverage. If PEG$_3$–PDMA were to be used as the physical coating in capillary zone electrophoresis, it could yield a well-suppressed eletroosmotic flow with greater stability and separate proteins with a lower relative standard deviation (RSD) of protein migration time and a higher separation efficiency than a bare fused-silica capillary in a broad pH range. © 2012 Wiley Periodicals, Inc. J. Appl. Polym. Sci. 129: 1179–1186, 2013

KEYWORDS: adsorption; coatings; proteins; separation techniques

Received 9 June 2012; accepted 4 September 2012; published online 27 November 2012

DOI: 10.1002/app.38559

INTRODUCTION

Protein adsorption is an important issue in many biorelated fields, including biomaterials, biomedical devices, and antibiofouling.[1–5] Nonspecific protein adsorption can degrade the sensitivity of diagnostic devices and cause a foreign-body inflammatory response in implanted biomaterials[6] and undesirable biofouling on ship hulls.[7] Methods to overcome nonspecific protein adsorption to surfaces have been developed. One direct and effective way is the modification of the surface with protein-resistant materials.[3] Various polymer materials, such as heparin,[8] dextran,[9] polyoxazolines,[10] poly(ethylene glycol) (PEG) or oligo(ethylene glycol),[11,12] and zwitterionic polymers,[13–16] have been used to physically modify the surface. Particularly, PEG-based materials with excellent nonfouling capabilities and biocompatibility have been used widely.[17,18] Several models have been proposed to explain the protein-resistance mechanism of PEG, including the steric repulsion model[19] for long PEG chains and the water barrier model[20] for short PEG or oligo(ethylene glycol) chains. Theoretical studies have indicated that an increase in the surface density of PEG chains will improve the protein-resistance capabilities.[21–23] Surface coverage is also an important parameter in determining the ability of a polymer layer.

Capillary zone electrophoresis (CZE) is a powerful analytical technique for large biopolymers, but protein adsorption on the negatively charged surface of fused-silica capillaries limits its application for protein separation. Physically absorbed polymer coatings could adsorb on the capillary inner surface via electrostatic, hydrogen bonding, or hydrophobic interactions, which have been proven to be effective in solving this problem and have the following advantages: simplicity of coating formation, the possibility of coating regeneration, and prior knowledge of the coating properties.[24–27]

In previous studies, poly(*N,N*-dimethyl acrylamide) (PDMA) showed a good self-coating ability to separate proteins in CZE as a physical coating, but the separation efficiency has been low because of the hydrophobic interactions between protein and the methyl groups of PDMA.[28,29] Therefore, we designed a star polymer with multiple PEG arms and one PDMA arm, expecting to obtain a greater PEG chain density and stability.

The synthesis methods of star-shaped polymers having poly(ethylene oxide) components include arm-first and core-first procedures.[30] In this study, a small-molecular linker, citric acid, was chosen to react with functional PEG arms in an arm-first procedure, and the PDMA arm was formed through atom-transfer radical polymerization (ATRP). The defined polymer

Applied Polymer SCIENCE

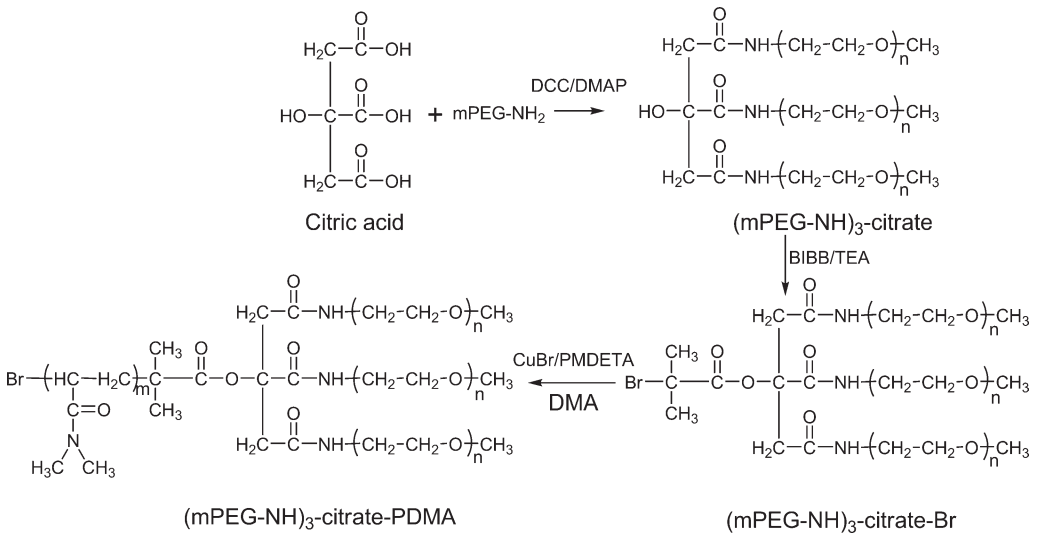

Scheme 1. Synthetic path of the star polymer $(mPEG\text{-}NH)_3$–citrate–PDMA.

structure was characterized by ^{1}H-NMR and IR spectroscopy and gel permeation chromatography (GPC). By use of a quartz crystal microbalance with dissipation (QCM-D) and CZE, we investigated the physical coating process and protein-resistance ability of PEG, PEG–PDMA, and PEG_3–PDMA in real time. The star polymer was used as a physical coating for separation proteins in CZE in a further study of its biological applications.

EXPERIMENTAL

Materials

All of the water used was deionized water (Lan Lan Water Co., Hefei, China) and was distilled three times by an SZ-3 automatic triple-pure water distiller (Shanghai Huxi Analysis Instrument Factory, Shanghai, China) before use. Dicyclohexylcarbodiimide, tetrahydrofuran, CH_2Cl_2, citric acid monohydrate (CAM), triethylamine (TEA), benzyl alcohol, phosphate, acetic acid, and sodium phosphate dibasic were obtained from SCRC (Shanghai, China).

2-Bromoisobutyryl bromide (BIBB), pentamethyldiethylenetriamine (PMDETA), 4-(dimethylamino) pyridine, PEG monomethyl ether (monomethoxy poly(ethylene glycol) (mPEG)-OH/PEG_{44}, 2000 g/mol, degree of polymerization (DP) $\approx$ 44), and *N,N*-dimethyl acrylamide (DMA) were purchased from Aldrich (St. Louis, MO, USA). DMA was distilled under reduced pressure before use. mPEG-OH was dried by azeotropic distillation with toluene before use. The block copolymer PEG_{44}–$PDMA_{22}$ was prepared in the following the way as reported by Xu et al.[31] Lysozyme from egg white (pI = 11.1, relative molecular mass (M_r) = 14,300), cytochrome c from horse heart (pI = 10.2, M_r = 12,400), ribonuclease A from bovine pancreas (pI = 9.3, M_r = 13,700), myoglobin from equine skeletal muscle (pI = 7.0, M_r = 17,800), α-chymotrypsinogen A from bovine pancreas (pI = 9.2, M_r = 25,656), trypsin inhibitor from soybean (pI = 6.2, M_r = 22,000), and fibrinogen (pI = 5.5, M_r = 340 000) were purchased from Sigma Chemicals (St. Louis, MO).

Physiological phosphate-buffered saline (PBS; 0.1*M*, pH 7.4) was prepared by the dilution of a mixture of Na_2HPO_4 (9.5 mL, 0.2*M*) and KH_2PO_4 (40.5 mL, 0.2*M*) to 0.1*M*. Each protein solution (1.0 mg/mL) was prepared by dissolution of the protein in PBS. The other reagents were used as received.

Synthesis and Characterization of $(mPEG\text{-}NH)_3$–Citrate–PDMA

The terminal hydroxyl groups of the mPEG-OH were first converted into amino groups to obtain $mPEG\text{-}NH_2$ according to the synthetic pathway reported by Zalipsky et al.[32] and Zeng et al.[33] The synthetic path of the star polymer is displayed in Scheme 1. First, $(mPEG\text{-}NH)_3$–citrate was synthesized by direct amidation between citric acid and $mPEG\text{-}NH_2$ as Ben-Shabat et al.[34] reported. $mPEG\text{-}NH_2$ (0.6 mmol, 0.126 g), citric acid (0.2 mmol, 38.4 mg), dicyclohexylcarbodiimide (0.72 mmol, 150 mg), and 4-(dimethylamino) pyridine (6 mg) were dissolved in CH_2Cl_2/tetrahydrofuran (1:1 v/v) and kept under stirring at room temperature for 1 day under dry conditions. The purification of the crude product was done by column chromatography (silica 60, 120 mesh) with a 1:1 mixture of ethyl acetate and methanol as the eluent. The purified product $(mPEG\text{-}NH)_3$–citrate was characterized by aqueous GPC and Fourier transform infrared (FTIR) spectroscopy. Then, $(mPEG\text{-}NH)_3$–citrate, BIBB, and TEA at a molar ratio of 1:1.2:1.8 were dissolved in CH_2Cl_2 and stirred for 6 h under ice–water bath conditions to get the ATRP macroinitiator $(mPEG\text{-}NH)_3$–citrate–Br. DMA, $(mPEG\text{-}NH)_3$–citrate–Br, CuBr, and PMDETA at a molar ratio of 50:1:1:1 were dissolved in toluene and added to a dried glass tube. The mixture was degassed by three freeze–pump–thaw cycles. Then, the tube was sealed *in vacuo* and immersed in a water bath thermostated at 30°C for 6 h. The reaction mixture was dialyzed for 72 h in water and then freeze-dried to obtain the final product, $(mPEG\text{-}NH)_3$–citrate–PDMA.

The IR spectra were recorded in the solid state with KBr pellets. A MAGNA-IR 750 instrument (Nicolet Instruments, Madison, WI, USA) was used to record the spectra in the range 400–4000 cm^{-1}. ^{1}H-NMR spectra were obtained in an AV-300 NMR spectrometer (Bruker BIOSPIN AG, Fällanden, Switzerland), and $CDCl_3$ was used as the solvent.

The number-average molecular weight (M_n), weight-average molecular weight (M_w), and polydispersity index were determined by GPC measurements (LC-10AVP HPLC system, Shimadzu, Kyoto, Japan). The mobile phase was an aqueous solution of 0.1*M* $NaNO_3$ with a flow rate of 1.00 mL/min at 40°C; a poly (ethylene oxide) standard was used for calibration.

QCM-D Measurements

The quartz crystal microbalance (QCM) has been widely used to measure the mass of material/molecules attached to the surface of crystals via changes in the frequency (Δf's).[35,36] In this study, the QCM-D with an AT-cut quartz crystal with a fundamental resonant frequency (f_a) of 5 MHz and a diameter of 14 mm was from Q-Sense AB (BiolinScientific, Vðstra Frälunda, Sweden). f_a of the quartz crystal decreases when a thin film is attached to it. If the film is thin and rigid, the decrease in frequency is proportional to the mass of the film (Δm). The mass of the adhering layer can be calculated with the Sauerbrey relation

$$\Delta m = -C\frac{\Delta f}{n} \quad (1)$$

where C is the mass sensitivity constant and n (= 1, 3…) is the overtone number. For the $f = 5$ MHz quartz crystal used in this experiment, $C = 17.7$ ng cm^{-2} Hz^{-1}. All of the presented data are from the third overtone ($n = 3$).

The SiO_2-coated resonator was boiled in a perhydrol and sulfuric acid mixture first for 15 min to get hydroxylation and to clean it; then, it was flushed with deionized water. After that, the resonator was dried by nitrogen and cleaned with reactive oxygen plasma. Polymer solutions were prepared by the dissolution of the polymers in PBS to the desired concentration (0.1%, m/v). Different proteins, including lysozyme, ribonuclease A, and fibrinogen dissolved in PBS (1 mg/mL), were used to investigate the protein-resistance properties of the coatings.

Coating Procedure. The SiO_2-coated resonator was rinsed with PBS until it reached equilibrium and f_a came to a steady value; then, we reset the value to 0. After that, the resonator was flushed with the polymer solution for 10 min and left to remain still for 10 min. The coated resonator was rinsed with PBS for 10 min to wash off remaining uncoated polymer, and f_a of the polymer-coated resonator was measured. In this case, Δf_p is the change in the resonant frequency ($f_a - 0$) by which the adsorption mass of the polymer could be calculated through the Sauerbrey relation.

Proteins Adsorption Procedure. After the coating procedure, the polymer-coated resonator was rinsed with the protein solution, and the resonant frequency was measured after the system stayed still for 10 min (f_b). Δf_a is the change $f_b - f_a$ by which the adsorption mass of the protein could be calculated. So we chose Δf_a as the indicator of nonspecific protein adsorption of the coating. Different polymer coatings and proteins adsorption processes were used with the same procedure as previously. All of the experiments were performed at 25°C.

CZE Experiments

All of the CZE experiments were carried out on a Beckman P/ACE MDQ capillary electrophoresis system (Beckman Coulter Instruments, Brea, UA, USA) with an ultraviolet–visible detector working at 214 nm. The bare fused-silica capillaries were obtained from Yongnian Optic Fiber Plant (Hebei, China) with effective/total length of 30/40 cm and an *i.d./o.d.* of 75/365 μm.

Eletroosmotic Flow (EOF) Measurements. All of the EOF measurements were carried out at 25°C with benzyl alcohol (0.02% v/v) as a neutral marker according to the procedure reported by Williams[37] and Xu et al.[31] Polymer solutions were prepared by the direct dissolution of the polymers in relevant buffer to the desired concentration (0.2% m/v) and were then filtered through a Millipore membrane filter (0.22 μm pore size). The capillaries were rinsed with polymer solutions for 10 min and stayed still for 10 min. To wash off the uncoated polymer, the coated capillaries were rinsed with relevant buffer for 5 min. The EOF measurements were carried out with phosphate–citrate buffers at different pHs as follows: 9.9 m*M* Na_2HPO_4, 15.1 m*M* CAM at pH 3.17, 16.6 m*M* Na_2HPO_4, 11.7 m*M* CAM at pH 4.16, 21.4 m*M* Na_2HPO_4, 9.3 m*M* CAM at pH 5.28, 26.4 m*M* Na_2HPO_4, 6.8 m*M* CAM at pH 6.12; 34.8 m*M* Na_2HPO_4, 2.6 m*M* CAM at pH 7.23, 39.0 m*M* Na_2HPO_4, and 0.5m*M* CAM at pH 8.26.

Protein-Separation Experiments. All of the protein solution (0.3 mg/mL) was injected for 5 s at 3447.5 Pa. The applied voltage was 20 kV. Before separation, the coated capillary was rinsed with buffer for 5 min and had a prerunning of 5 min. After each separation, the capillaries were flushed with buffer for 10 min to remove the adsorbed proteins. The capillaries were recoated when the buffer was changed. Three kinds of proteins (lysozyme, ribonuclease A, and cytochrome c) were separated in phosphate–citrate buffer at different pHs: 3.17, 4.16, 5.28, and 6.12. The protein mixture, including lysozyme, ribonuclease A, cytochrome c, myoglobin, α-chymotrypsinogen A, and trypsin inhibitor, was separated at pH 3.17.

RESULTS AND DISCUSSION

Characterization of the Star Polymer PEG_3–PDMA

Products during the reaction process were characterized by ^{1}H-NMR and IR spectroscopy and GPC. Figure 1 reveals the representative FTIR spectra of $(mPEG\text{-}NH)_3$–citrate, $(mPEG\text{-}NH)_3$–citrate–Br, and $(mPEG\text{-}NH)_3$–citrate–PDMA. The absorption band at 1645 cm^{-1} [Figure 1(a)] indicates that an amidation reaction occurred. After $(mPEG\text{-}NH)_3$–citrate reacted with BIBB, there was a new absorption band above 1700 cm^{-1} [Figure 1(b)], which indicated the formation of $(mPEG\text{-}NH)_3$–citrate–Br. Then, after the polymerization, there was a wide adsorption band at 1636 cm^{-1} [Figure 1(c)] corresponding to the amido bond of PDMA. Table I shows the GPC results of PEG and $(mPEG\text{-}NH)_3$–citrate. The ratio of M_n of $(mPEG\text{-}NH)_3$–citrate to M_n of mPEG was 2.8 : 1. Figure 2 shows ^{1}H-NMR spectrum of $(mPEG\text{-}NH)_3$–citrate–Br in $CDCl_3$. According to the integral area of the peaks {$\delta = 3.41$ (a, —OCH_3) and $\delta = 1.96$ [b, —$C(CH_3)_2$]}, the number of PEG arms could be calculated, and the result indicates that a three-armed polymer was successfully prepared.

The ^{1}H-NMR spectroscopy of the final product, PEG_3–PDMA (resolved in $CDCl_3$), is shown in Figure 3 on the basis of the

Applied Polymer SCIENCE

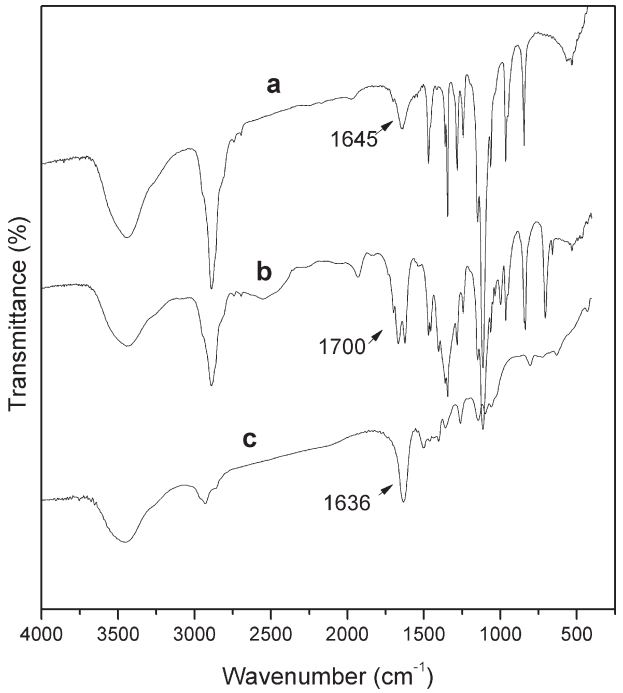

Figure 1. FTIR spectra of (a) $(mPEG\text{-}NH)_3$–citrate, (b) $(mPEG\text{-}NH)_3$–citrate–Br, and (c) $(mPEG\text{-}NH)_3$–citrate–PDMA.

following signal assignment: δ (ppm): 3.66 (a, —CH_2—CH_2—O—), 2.93 [b, $N(CH_3)_2$], 2.66 (c, —CH—CH_2—), 2.45 (d, —CH_2—C=O), 1.31 [e, —$C(CH_3)_2$—C=O], and 1.75 (f, —C—CH_2—). The DP of the PDMA block was 24; this was calculated according to the integral area of the peaks $\delta = 3.66$ (CH_2, PEG) and $\delta = 2.93$ [—$N(CH_3)_2$, DMA]. All of the results demonstrate that a well-defined four-armed polymer, $(PEG_{44})_3$–$PDMA_{24}$, was obtained.

Surface Adsorption and Protein-Resistance Behavior Investigation

A baseline was recorded for the QCM-D instrument before the introduction of the polymers to the SiO_2-coated resonator, and the resulting adsorption was monitored. Figure 4 shows the star polymer $(PEG_{44})_3$–$PDMA_{24}$ coating and fibrinogen adsorption process and reveals the specific procedures for all of the QCM experiments. The constant Δf from the beginning indicated that the system reached equilibrium after it was flushed with PBS for several minutes. Then, the resonator was rinsed with the star polymer solution for 10 min, and Δf decreased and ΔD increased significantly. This indicated polymer adsorption on the SiO_2-coated resonator surface. Δf became constant after the polymer-coated resonator was rinsed with PBS for 10 min to wash away the uncoated polymer, which meant that a steady polymer coating was formed, and Δf_p was measured.

Table I. GPC Results of PEG and PEG_3–Citrate

	M_n	M_n[b]	M_w[b]	M_w/M_n[b]
PEG	2000[a]	2085	2189	1.05
PEG_3-citrate	6138[c]	5881	8586	1.46

[a]Molar mass as Aldrich presented, [b]Molar mass obtained from GPC, [c]Molar mass obtained by theoretical calculation.

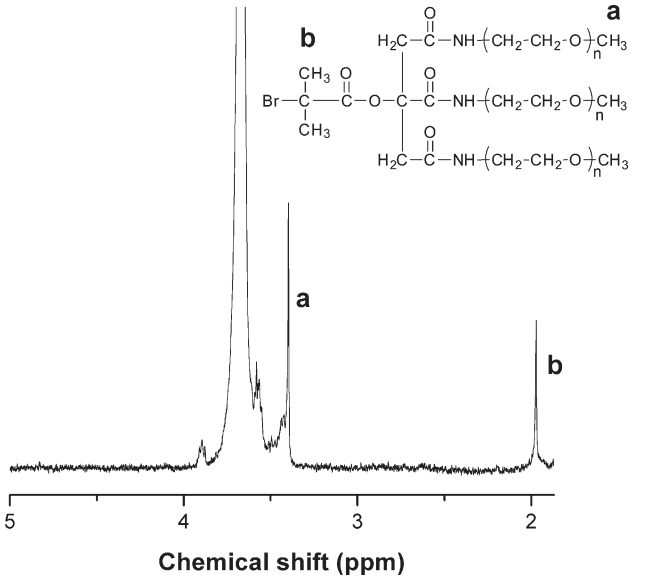

Figure 2. ^{1}H-NMR spectrum of $(mPEG\text{-}NH)_3$–citrate–Br in $CDCl_3$.

After the coating process, various proteins with different values of the *isoelectric point* (pI), a critical pH point at which a protein carries no net electrical charge, were used to quantitatively evaluate the protein adsorption on the polymer-coated resonator surfaces. The changes in the frequency (Δf) and dissipation (ΔD) gave information about the protein adsorption and structural changes in the protein layer, as mentioned previously. As shown in Figure 4, for the $(PEG_{44})_3$–$PDMA_{24}$ coating, Δf decreased and ΔD increased slightly when the fibrinogen solution was added. The total nonspecific adsorption of proteins on the different polymer-coated surfaces could be calculated by Δf_a.

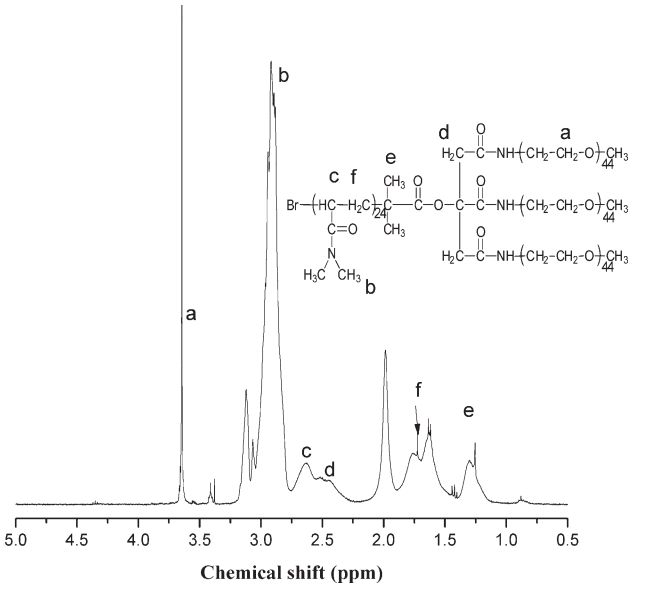

Figure 3. ^{1}H-NMR spectrum of the star polymer $(PEG_{44})_3$–$PDMA_{24}$ in $CDCl_3$.

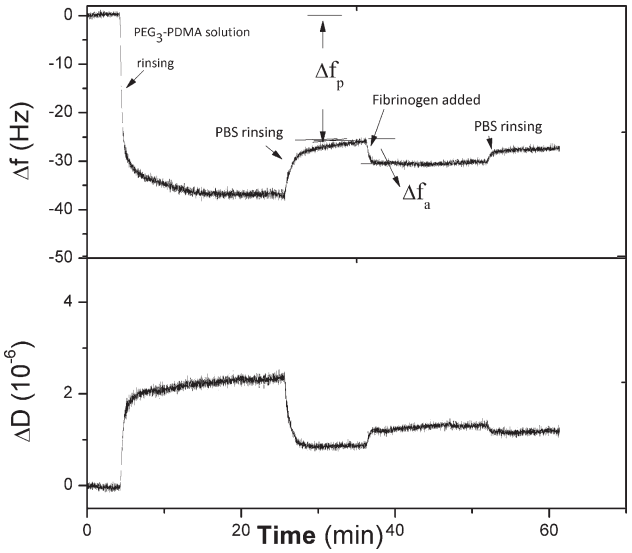

Figure 4. Time dependence of Δf and ΔD for the $(PEG_{44})_3$–$PDMA_{24}$ coating and fibrinogen adsorption on the $(PEG_{44})_3$–$PDMA_{24}$ surface at 25°C.

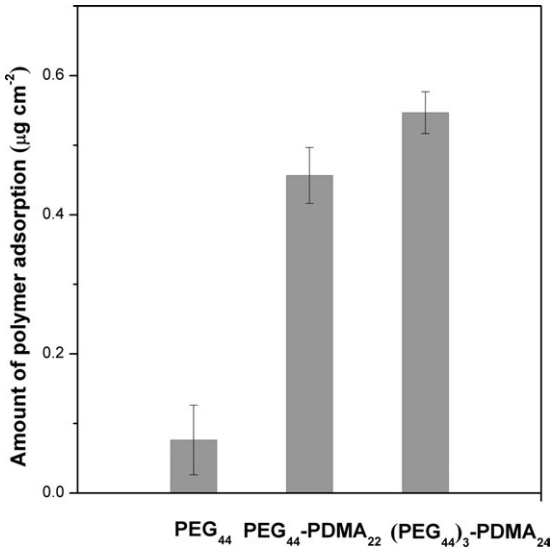

Figure 5. Physical adsorption of PEG_{44}, PEG_{44}–$PDMA_{22}$ and $(PEG_{44})_3$–$PDMA_{24}$ with the same concentration (0.1% mol/v) on the SiO_2-coated resonator surface at 25°C. The data are the mean plus or minus the standard deviation ($n = 3$).

Figure 5 shows the physical adsorption amount of the different polymers on the SiO_2-coated resonator surface. As is well known, PEG can interact with the silica surface via hydrogen bonding between the ether oxygen of PEG and the silanol groups. However, in the PBS buffer (pH 7.4), hydrogen-bonding interaction is weakened. So PEG could be easily flushed away by PBS and could not form a stable polymer layer. In contrast, polymers with PEG and PDMA chains could interact with the

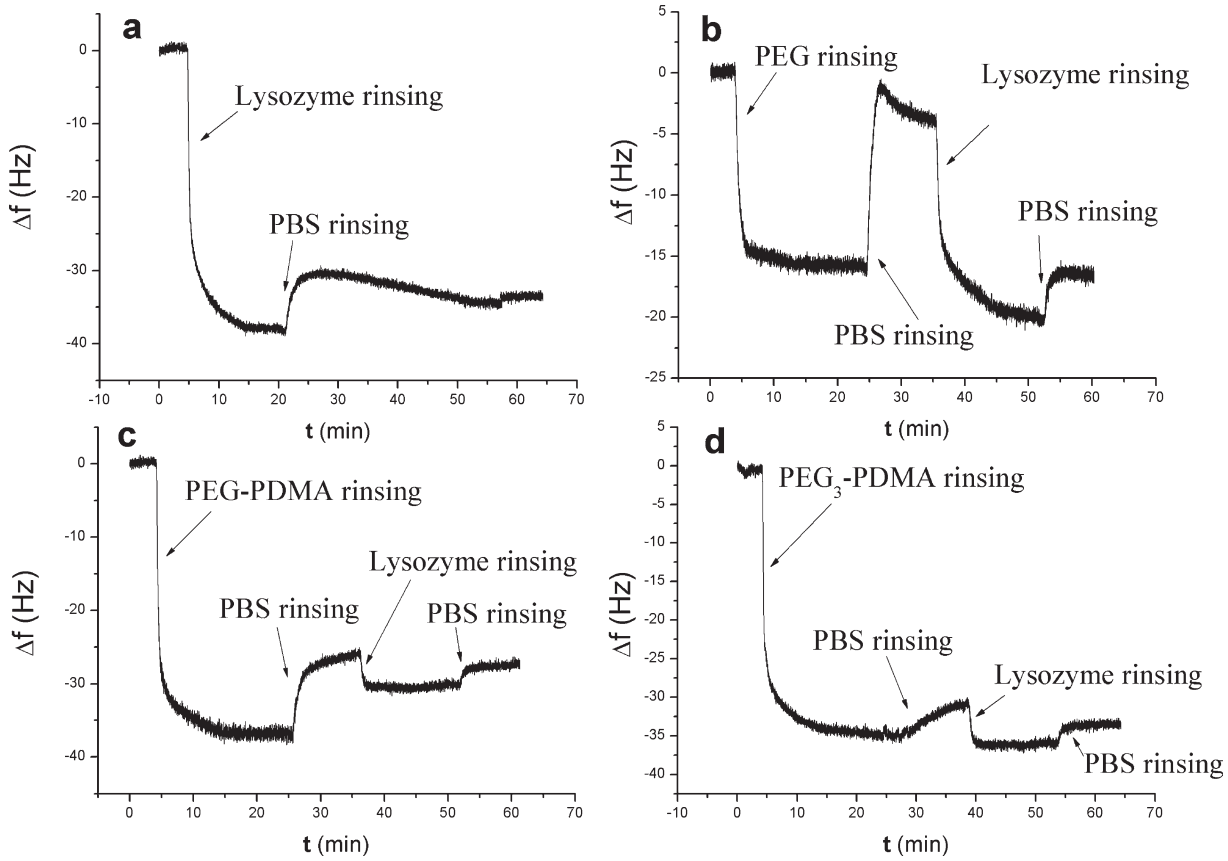

Figure 6. Time (t) dependence of Δf for the polymer coating and lysozyme adsorption on the (a) SiO_2, (b) PEG_{44}, (c) PEG_{44}–$PDMA_{22}$, and (d) $(PEG_{44})_3$–$PDMA_{24}$ surface at 25°C.

Applied Polymer SCIENCE

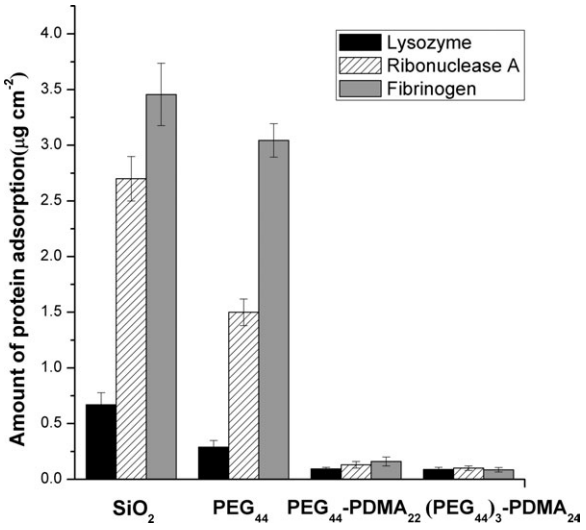

Figure 7. Amounts of various proteins (lysozyme, ribonuclease A, and fibrinogen) adsorbed on the SiO_2, PEG_{44}, PEG_{44}–$PDMA_{22}$, and $(PEG_{44})_3$–$PDMA_{24}$ surfaces at 25°C. The data are the mean plus or minus the standard deviation ($n = 3$).

surface by both hydrogen bonding and hydrophobic interaction between the polymers and the silica surface and thus obtain a long-term stability. Compared to PEG_{44}–$PDMA_{22}$ (adsorption = 0.46 ± 0.04 $\mu g/cm^2$) and $(PEG_{44})_3$–$PDMA_{24}$ (adsorption = 0.55 ± 0.03 $\mu g/cm^2$), $(PEG_{44})_3$–$PDMA_{24}$ showed an even better self-coating ability and had a greater PEG chain density, which could be calculated from the adsorption amount.

Figure 6 shows the lysozyme adsorption process on the SiO_2-, PEG_{44}-, PEG_{44}–$PDMA_{22}$-, and $(PEG_{44})_3$–$PDMA_{24}$-coated resonator surfaces. For the SiO_2 surface, the lysozyme adsorption process was gradual for a long time, and the adsorption amounts were huge. The PEG_{44} coating did not show good results because of its unsteady property in PBS, and this led to a low surface coverage. In contrast, for the PEG_{44}–$PDMA_{22}$- and $(PEG_{44})_3$–$PDMA_{24}$-coated surfaces, the lysozyme adsorption processes were short (<2 min), and f_a remained constant for the next 8 min; this indicated that both of the polymers had excellent protein-resistance properties. The same phenomenon was repeated for other protein adsorptions.

As shown in Figure 7, lysozyme, ribonuclease A, and fibrinogen were used for protein-resistance investigations of the SiO_2-, PEG_{44}-, PEG_{44}–$PDMA_{22}$-, and $(PEG_{44})_3$–$PDMA_{24}$-coated surfaces. Fibrinogen, a component in blood typically thought to be important in the inflammatory response, is commonly used to evaluate the nonfouling characteristics of surfaces. The adsorption amounts of fibrinogen on the PEG_{44}–$PDMA_{22}$ and $(PEG_{44})_3$–$PDMA_{24}$ surfaces were shown to be 0.16 ± 0.04 and 0.09 ± 0.02 $\mu g/cm^2$, respectively. Compared with the fibrinogen adsorption on the SiO_2 surface (3.46 ± 0.28 $\mu g/cm^2$), both of them showed excellent fibrinogen resistance.

For the basic proteins lysozyme and ribonuclease A, the PEG_{44}–$PDMA_{22}$ and $(PEG_{44})_3$–$PDMA_{24}$ coatings also presented remarkable protein-resistance abilities, which could reduce the adsorption to 13% at least compared with the SiO_2 surface. Compared with the adsorption amount of ribonuclease A on the PEG_{44}–$PDMA_{22}$-coated surface (0.16 ± 0.04 $\mu g/cm^2$), the $(PEG_{44})_3$–$PDMA_{24}$-coated surface presented better performance (0.08 ± 0.02 $\mu g/cm^2$). These results demonstrate that the polymer coating ability was greatly enhanced with PDMA chains, and the star polymer with a higher PEG chain density showed better protein-resistance properties; this showed its certain application prospects in biomedical devices and food analysis.

Application in CZE

EOF Measurements. The migration velocity of an ionic species is the sum of its electrophoretic velocity and EOF velocity in CZE. EOF plays the role of a driving force, and the difference in the electrophoretic mobility causes different migration times. For bare capillaries, the adsorption of a protein onto the capillary inner wall alters the EOF velocity by altering the ζ potential of the surface, which causes changeable migration times for protein separation. To solve this problem, capillaries coated with the polymers summarized in the Introduction are widely used and exhibit a steady and well-suppressed EOF.

As shown in Figure 8, EOF measurements were carried out in a bare fused-silica capillary and PEG_{44}-, PEG_{44}–$PDMA_{22}$-, and $(PEG_{44})_3$–$PDMA_{24}$-coated capillaries at different pH values with the same experimental approach. For the bare fused-silica capillary, EOF was toward the negative electrode and exhibited a positive value. It sharply increased as the pH increased because of the dissociation of silanol groups. So the bare capillary was not suitable for acid–protein separation at high pHs. PEG can form a more stable coating under acid conditions and exhibit a lower EOF because of the enhancement of the hydrogen-bonding interaction.[38–40] However, the dissociation of silanol groups made the interaction weaken as the pH increased, which presented incremental EOFs. In contrast, the PEG_{44}–$PDMA_{22}$ and $(PEG_{44})_3$–$PDMA_{24}$ coating stably suppressed EOF with lower

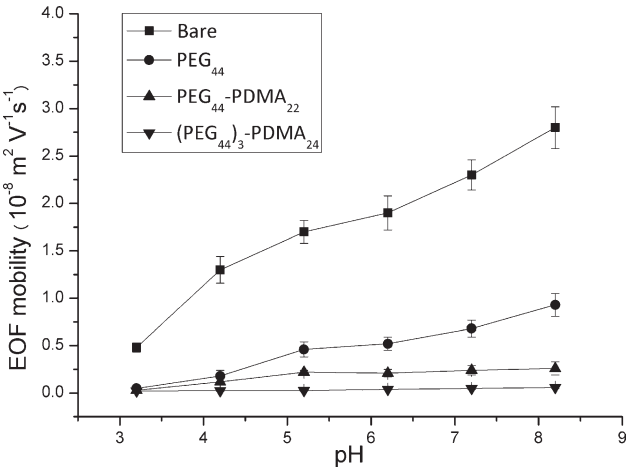

Figure 8. Effect of the buffer pH on EOF. A comparison among a bare fused-silica capillary, PEG_{44}-, PEG_{44}–$PDMA_{22}$-, and $(PEG_{44})_3$–$PDMA_{24}$-coated capillaries. Conditions: capillary *i.d./o.d.* = 75/365 μm and effective/total length = 30/40 cm, temperature = 25°C, applied voltage = 10 kV for 1 min, injection = 1379 Pa for 3 s, buffer = phosphate–citrate (pH 3.22–8.21). The data are the mean plus or minus the standard deviation ($n = 3$).

Table II. Repeatability of the Migration Time and Peak Efficiency Results for Consecutive Runs ($n = 3$) of Three Basic Proteins at Different pHs[a] in the $(PEG_{44})_3$–$PDMA_{24}$-Coated Capillary[b]

	pH 3.17			pH 4.16			pH 5.28			pH 6.12		
Protein	*t* (min)	RSD (%)[c]	*N* (m^{-1})[d]	*t* (min)	RSD (%)[c]	*N* (m^{-1})[d]	*t* (min)	RSD (%)[c]	*N* (m^{-1})[d]	*t* (min)	RSD (%)[c]	*N* (m^{-1})[d]
Cytochrome c	2.90	0.3	182,500	3.91	0.2	70,100	7.01	1.2	65,030	7.20	2.1	94,000
Lysozyme	3.07	0.4	151,200	3.97	0.2	88,810	6.44	0.7	83,321	6.46	1.3	77,000
Ribounclease A	3.65	0.5	133,630	5.27	0.6	97,400	11.67	1.1	60,650	12.93	1.4	112,000

t, time.
[a]Separation buffer: phosphate–citrate at pH 3.17, 4.16, 5.28, and 6.12, [b]Conditions: capillary *i.d./o.d.* = 75/365 μm and effective/total length = 30/40 cm, temperature = 25°C, separation voltage = 20 kV; detection, UV = 214 nm, injection = 3.45 kPa for 5 s, polymer concentration = 0.2% m/v, sample = 0.5 mg/mL of a three-protein mixture, [c]RSD of migration time (three consecutive measurements), [d]*N*, theoretical plate number of the protein peak.

relative standard deviation (RSD) over the pH range 3.17–8.21; this means that polymers with PDMA chains could adsorb onto the capillary inner surface tightly. Compared PEG_{44}–$PDMA_{22}$, the $(PEG_{44})_3$–$PDMA_{24}$-coated capillary with lower EOF (10^{-10} m^2 V^{-1} s^{-1}) yielded a more stable physically absorbed coating on the capillary inner wall over a wide pH range; this indicated its better coating ability. A steady EOF makes it possible to separate proteins in different buffer conditions for further study.

Effect of pH on the Separation of Basic Proteins. To investigate the applicability of the star polymer $(PEG_{44})_3$–$PDMA_{24}$ coating, separations of three standard basic proteins (cytochrome c, lysozyme, and ribonuclease A) were performed in a broad pH range. As shown in Table 2, the migration time of the proteins increased as the buffer pH increased. Because the charge of the basic proteins was positive in the pH range (3.17–6.12) and decreased at higher pHs (which resulted in a reduction in the electrophoretic mobility), it presented a longer migration time. At pH 4.16 and 5.28, there was a migration order switch between cytochrome c and lysozyme. Because the surface charge and conformational properties of the proteins were strongly dependent on the pH value and the composition of the buffer, the switch implied that pI of the proteins could not be the indicator of simply the migration time order.

For the $(PEG_{44})_3$–$PDMA_{24}$-coated capillary, basic proteins could be separated with moderate peak efficiency ($>10^4$ m^{-1}) and a low RSD of migration time (<2.1%) at pH 3.17–6.12. Better performance was obtained at pH 3.17 with a lower RSD (<0.5%); this indicated that optimal separation conditions needs to be explored for a high separation efficiency. Better separation conditions need to be explored in a future study to obtain a higher separation efficiency.

Separation of the Protein Mixture. The $(PEG_{44})_3$–$PDMA_{24}$-coated capillary was used to separate the protein mixture for further application study, which included basic, acid, and neutral proteins. As shown in Figure 9, the bare fused-silica capillary could not separate the protein mixture effectively because of a serious protein adsorption problem, which caused a tailing of the sample peak and even a missing peak. Protein adsorption caused an unsteady EOF and changeable protein migration time. In contrast, the $(PEG_{44})_3$–$PDMA_{24}$-coated capillary clearly showed peaks of six proteins with a greater separation efficiency and indicated that the star polymer coating could resist protein adsorption effectively and had a great stability for protein separation.

CONCLUSIONS

A star polymer, $(PEG_{44})_3$–$PDMA_{24}$, was successfully synthesized by amidation and ATRP with a defined structure; this was demonstrated by ^{1}H-NMR and IR spectroscopy and GPC. The protein-resistance behaviors of different polymer-coated surfaces were investigated by the use of QCM-D. $(PEG_{44})_3$–$PDMA_{24}$ and PEG_{44}–$PDMA_{22}$ had a better physical coating ability than PEG because of the hydrophobic interactions between the PDMA chain and the silica surface. $(PEG_{44})_3$–$PDMA_{24}$, with a higher

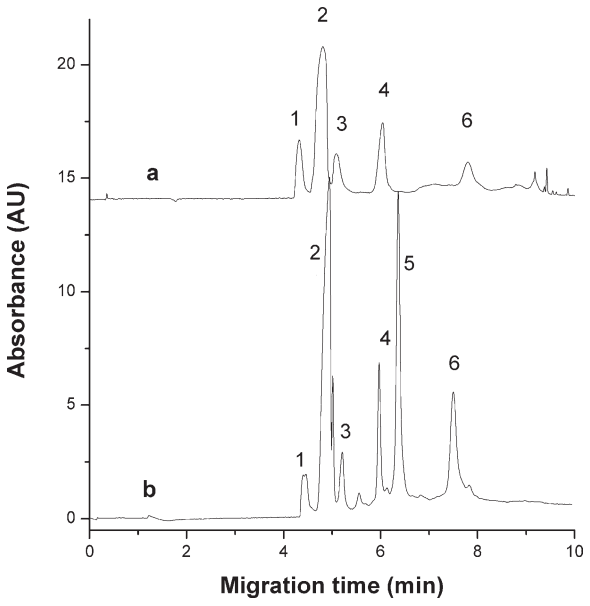

Figure 9. Electropherograms of a mixture of neutral, acidic, and basic proteins. (a) Comparison between a bare fused-silica capillary and (b) a $(PEG_{44})_3$–$PDMA_{24}$-coated capillary. Separation buffer: phosphate–citrate of pH 3.17. Peak identification: (1) cytochrome c, (2) lysozyme, (3) myoglobin, (4) ribonuclease A, (5) a-chymotrypsinogen A, and (6) trypsin inhibitor. Conditions: capillary *i.d./o.d.* = 75/365 μm and effective/total length = 30/40 cm, temperature = 25°C, separation voltage = 15 kV, detection: UV = 214 nm; injection = 3.45 kPa for 5 s, polymer concentration = 0.2% m/v. Sample = 0.3 mg/mL of a six-proteins mixture.

PEG chain density, showed a better protein-resistance ability than the diblock polymer.

For further study of its biological application, we used $(PEG_{44})_3$–$PDMA_{24}$ as a physical coating for protein separation by CZE. The preparation of the coating was simple, reproducible, and convenient for duplicate experiments. With good stability on the inner surface, the $(PEG_{44})_3$–$PDMA_{24}$ coating suppressed EOF effectively over the pH range 3.22–8.21 and separated different proteins simultaneously with moderate efficiency and a great migration time repeatability; this indicated its potential for biological sample separation.

ACKNOWLEDGMENT

The authors gratefully acknowledge Xiaowen Wang for an introduction to the technique of QCM-D and Guangming Liu for relevant discussions concerning the QCM results. This research was supported by the National Natural Science Foundation of China (grant number 21074124) and the Ministry of Science and Technology of China (grant number 2012CB933802).

REFERENCES

1. Lee, J. H.; Ju, Y. M.; Kim, D. M. *Biomaterials* **2000**, *21*, 683.
2. Williams, D. F. *Biomaterials* **2008**, *29*, 2941.
3. Werner, C.; Maitz, M. F.; Sperling, C. J. *Mater. Chem.* **2007**, *17*, 3376.
4. Senaratne, W.; Andruzzi, L.; Ober, C. K. *Biomacromolecules* **2005**, *6*, 2427.
5. Wisniewski, N.; Reichert, M. *Colloid Surf. B* **2000**, *18*, 197.
6. Thomsen, P.; Gretzer, C. *Curr. Opin. Solid State Mater. Sci.* **2001**, *5*, 163.
7. Chambers, L. D.; Stokes, K. R.; Walsh, F. C.; Wood, R. J. K. *Surf. Coat. Techno.* **2006**, *201*, 3642.
8. Johnell, M.; Larsson, R.; Siegbahn, A. *Biomaterials* **2005**, *26*, 1731.
9. Delgado, A. D.; Leonard, M.; Dellacherie, E. *Langmuir* **2001**, *17*, 4386.
10. Konradi, R.; Pidhatika, B.; Muhlebach, A.; Textort, M. *Langmuir* **2008**, *24*, 613.
11. Prime, K. L.; Whitesides, G. M. *J. Am. Chem. Soc.* **1993**, *115*, 10714.
12. Roberts, C.; Chen, C. S.; Mrksich, M.; Martichonok, V.; Ingber, D. E.; Whitesides, G. M. *J. Am. Chem. Soc.* **1998**, *120*, 6548.
13. Chen, S. F.; Yu, F. C.; Yu, Q. M.; He, Y.; Jiang, S. Y. *Langmuir* **2006**, *22*, 8186.
14. Holmlin, R. E.; Chen, X. X.; Chapman, R. G.; Takayama, S.; Whitesides, G. M. *Langmuir* **2001**, *17*, 2841.
15. Ladd, J.; Zhang, Z.; Chen, S.; Hower, J. C.; Jiang, S. *Biomacromolecules* **2008**, *9*, 1357.
16. Oishi, T.; Tanaka, H.; Yamasaki, H.; Onimura, K. *J. Appl. Polym. Sci.* **2002**, *86*, 1092.
17. Alcantar, N. A.; Aydil, E. S.; Israelachvili, J. N. *J. Biomed. Mater. Res.* **2000**, *51*, 343.
18. Wang, R. L. C.; Kreuzer, H. J.; Grunze, M. *J. Phys. Chem. B* **1997**, *101*, 9767.
19. Ostuni, E.; Kane, R.; Chen, C. S.; Ingber, D. E.; Whitesides, G. M. *Langmuir* **2000**, *16*, 7811.
20. Jeon, S. I.; Lee, J. H.; Andrade, J. D.; Degennes, P. G. *J. Colloid Interface Sci.* **1991**, *142*, 149.
21. Gombotz, W. R.; Guanghui, W.; Hoffman, A. S. *J. Appl. Polym. Sci.* **1989**, *37*, 91.
22. Unsworth, L. D.; Sheardown, H.; Brash, J. L. *Langmuir* **2008**, *24*, 1924.
23. Metzke, M.; Bai, J. Z.; Guan, Z. B. *J. Am. Chem. Soc.* **2003**, *125*, 7760.
24. Liu, H.; Shi, R. H.; Wan, W. M.; Yang, R. M.; Wang, Y. M. *Electrophoresis* **2008**, *29*, 2812.
25. Bernal, J.; Rodriguez-Meizoso, I.; Elvira, C.; Ibanez, E.; Cifuentes, A. *J. Chromatogr. A* **2008**, *1204*, 104.
26. Bernal, J.; Sanchez-Hernandez, L.; Elvira, C.; Velasco, D.; Ibanez, E.; Cifuentes, A. *J. Sep. Sci.* **2009**, *32*, 605.
27. Wang, A. J.; Witos, J.; D'Ulivo, L.; Vainikka, K.; Riekkola, M. L. *Electrophoresis* **2009**, *30*, 3939.
28. Chiari, M.; Cretich, M.; Damin, F.; Ceriotti, L.; Consonni, R. *Electrophoresis* **2000**, *21*, 909.
29. Madabhushi, R. S.; Vainer, M.; Dolnik, V.; Enad, S.; Barker, D. L.; Harris, D. W.; Mansfield, E. S. *Electrophoresis* **1997**, *18*, 104.
30. Lapienis, G. *Prog. Polym. Sci.* **2009**, *34*, 852.
31. Xu, J.; Yang, L. Y.; Luo, Z. F.; Wang, Y. M. *Electrophoresis* **2010**, *31*, 1713.
32. Zalipsky, S.; Gilon, C.; Zilkha, A. *Eur. Polym. J.* **1983**, *19*, 1177.
33. Zeng, R. J.; Luo, Z. F.; Zhou, D.; Cao, F. H.; Wang, Y. M. *Electrophoresis* **2010**, *31*, 3334.
34. Ben-Shabat, S.; Kumar, N.; Domb, A. *J. Macromol. Biosci.* **2006**, *6*, 1019.
35. Marx, K. A. *Biomacromolecules* **2003**, *4*, 1099.
36. Andersson, M.; Andersson, J.; Sellborn, A.; Berglin, M.; Nilsson, B.; Elwing, H. *Biosens. Bioelectron.* **2005**, *21*, 79.
37. Williams, B. A.; Vigh, C. *Anal. Chem.* **1996**, *68*, 1174.
38. Tran, N. T.; Taverna, M.; Miccoli, L.; Angulo, J. F. *Electrophoresis* **2005,** *26*, 3105.
39. Preisler, J.; Yeung, E. S. *Anal. Chem.* **1996**, *68*, 2885.
40. Iki, N.; Yeung, E. S. *J. Chromatogr. A* **1996**, *731*, 273.